ADVANCED MATERIALS INTERFACES
Open Access
www.advmatinterfaces.de

Ultra-Thin Metal Oxide Superstructure of Pd(001) as Passivation Interlayer at Organic/Metal Interface

Isheta Majumdar, Francesco Goto, Alberto Calloni,* Lamberto Duò, Franco Ciccacci, and Gianlorenzo Bussetti*

At organic molecule/metal interfaces for electronic applications, it is required of the metal surface to be passivated in view of preserving the molecular properties of the ordered organic layer. This can be achieved by screening the metal with a single atomic layer of O, namely, ultra-thin metal oxide (UTMO) layers. Cobalt tetraphenylporphyrins (CoTPP) on oxygen passivated Fe(001), with 1 ML O coverage, have revealed a molecule/substrate decoupling effect due to the formation of an ultra-thin Fe oxide layer at the interface. However, the threshold concentration of surface O required to observe the decoupling effect has not been assessed yet. In this work, the possibility of stabilizing different ultra-thin Pd oxide superstructures, characterized by a different number of O atoms per unit cell, is exploited to investigate the O decoupling effect on CoTPP films. Two Pd oxide superstructures are considered: Pd(001)-$p(2 \times 2)$O and Pd(001)-$p(\sqrt{5} \times \sqrt{5})$R27°O, with 0.25 and 0.80 ML O coverages, respectively, which are characterized by low-energy electron diffraction (LEED), X-ray and ultra-violet photoelectron spectroscopies (XPS/UPS) and inverse photoemission spectroscopy (IPES). The results suggest a lower limit of 0.80 ML O coverage as a passivation interlayer to obtain an ordered and decoupled CoTPP monolayer on Pd(001).

1. Introduction

The miniaturization of devices (such as transistors, switches, solar cells, etc.) has already reached the molecular length scale; the distance between electronic elements is ≈5 nm. This limit represents a problem for further improvements in, e.g., the device calculus power.[1] As a consequence, other strategies have been proposed in the last 50 years.[2,3] Among these, the employment of organic molecules, ordered onto a proper substrate is considered a viable strategy that, before a massive implementation, requires theoretical simulations and new experimental data. Organic molecules, when integrated into electronic devices (organic electronics), offer a better tunability of the transport properties w.r.t traditional silicon-based electronics.[4] In addition, organic molecules can be synthesized to show specific electronic and optical properties. For these reasons, ultra-thin organic films offer, in principle, the possibility of a bottom-up fabrication of 2D scalable devices.[5] However, this preparation protocol finds a serious bottleneck when molecules are deposited onto technologically relevant substrates, such as silicon, as well as on metal contacts. In fact, the reactivity of these substrates is strong enough to perturb the deposited molecules by altering their morphology, electronic levels, and optical properties. This effect, widely known as the surface ligand effect, prescribes to consider the metal surface as a special ligand for the molecules and the interaction a sort of a new compound.[6] To overcome this limit, molecular spacers are usually employed for decoupling the deposited molecules from the buried substrate.[7] However, spacers can significantly alter the substrate properties (conductivity, magnetic properties, etc.). For this reason, thin or even ultra-thin metal oxide (UTMO) layers have been proposed as a viable alternative. We recently proved that even a single layer (1 ML) of O atoms on a highly reactive substrate, such as Fe, is able to preserve the main electronic features of porphyrins,[8–26] molecules that are widely employed also in functional devices.[27] Here, porphyrins have been chosen because they have a planar structure, which exposes the inner metal ion where the main interaction with the environment takes place, including the substrate surface when they lie flat on it. The porphyrins/substrate interaction is usually strong on metals used in electronic devices, thus making this system particularly suitable for finding strategies for efficient molecular decoupling at the interface.

The successful implementation of the UTMO decoupling interlayer at the porphyrins/Fe interface motivated us to extend the above research along two different lines: i) the first one seeks possible alternatives to the Fe surface; ii) the second one tries to evaluate the threshold concentration of O required to enable

I. Majumdar, F. Goto[+], A. Calloni, L. Duò, F. Ciccacci, G. Bussetti
Department of Physics
Politecnico di Milano
Leonardo da Vinci 32, Milan 20133, Italy
E-mail: isheta.majumdar@polimi.it; alberto.calloni@polimi.it

The ORCID identification number(s) for the author(s) of this article can be found under https://doi.org/10.1002/admi.202400443

[+]Present address: Institut National de la Recherche Scientifique – Énergie Matériaux Télécommunications, Varennes, Quebec J3X 1S2, Canada

DOI: 10.1002/admi.202400443

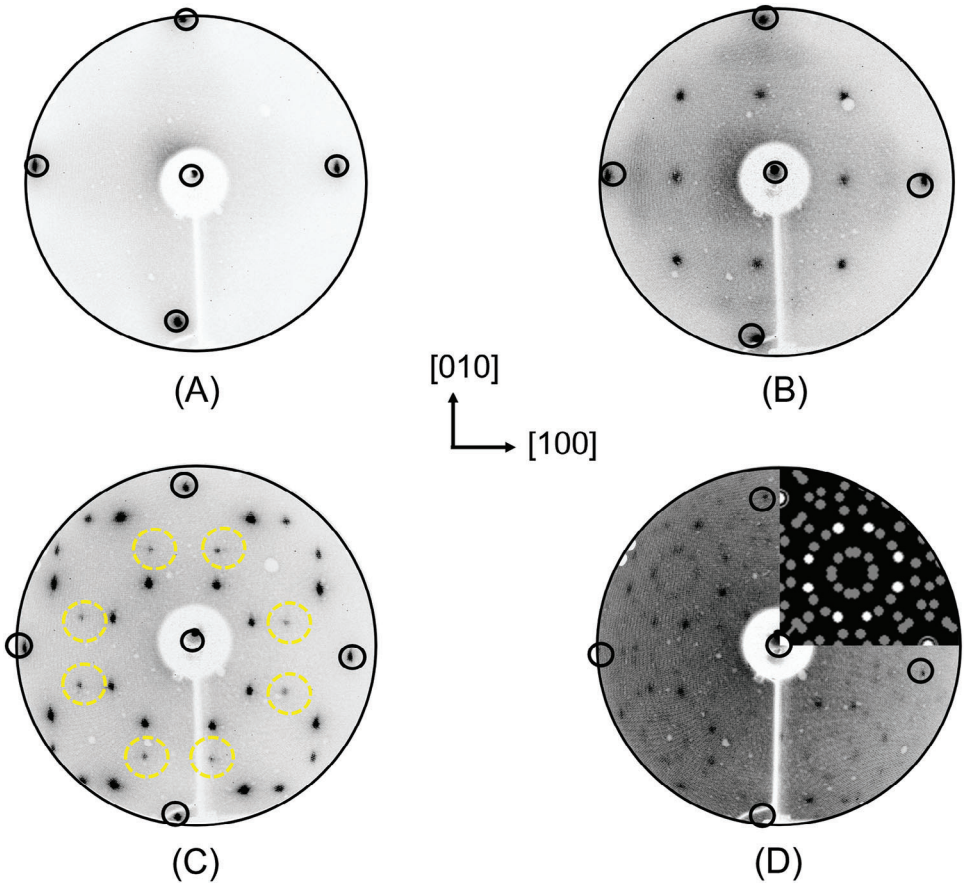

Figure 1. LEED negative images obtained at 55 eV beam energy for A) Pd(001)-$p(1\times1)$, B) Pd(001)-$p(2\times2)$O, C) Pd(001)-$p(\sqrt{5}\times\sqrt{5})$R27°O. The yellow circles highlight the diffraction spots that distinguish the presence of a single layer of Pd oxide, or $p(\sqrt{5}\times\sqrt{5})$R27°O phase. D) 1 ML CoTPP/Pd(001)-$p(\sqrt{5}\times\sqrt{5})$R27°O with a quadrant showing the corresponding simulated LEED pattern which is a mixed straight (5×5) and rotated (5×5)R37° pattern (see the text). In all panels, the black circled diffraction spots represent the diffraction from the underlying clean Pd(001)-$p(1\times1)$ substrate.

the decoupling effect. Regarding point (i), we previously demonstrated the crucial role of O in preserving the cobalt tetraphenylporphyrins (CoTPP) electronic features on Cu(110), although the quality of the molecular superstructure, judged by low energy electron diffraction (LEED), was very low.[28] In the present work, we achieve the porphyrins/substrate decoupling at an oxygen passivated Pd(001) surface with stronger evidence, something that has not been demonstrated before. Regarding point (ii), in the present work, we exploit the possibility of achieving two different surface ultra-thin metal oxide (UTMO) superstructures on the Pd(001) surface[29] with different O coverages, namely 0.25 ML and 0.80 ML.[30–38] Later, we estimate the minimum percentage of O atoms required for a full screening of molecules.

Both Fe(001) and Pd(001) surfaces expose the same square surface mesh with not very dissimilar lattice parameters: 2.86 Å for Fe(001) and 2.74 Å for Pd(001). Considering the structural similarities between Fe and Pd, the deposition of a monolayer of CoTPP molecules on the passivated Pd substrate can be directly compared to data collected on CoTPP / oxygen passivated Fe [Fe(001)-$p(1\times1)$O] interfaces,[18–22,25] wherein porphyrins are deposited on 1 ML O covered Fe substrates. As in our previous work, surface sensitive techniques such as LEED, X-ray, and ultra-violet photoelectron spectroscopies (XPS and UPS, respectively), and inverse photoemission spectroscopy (IPES) have been utilized to assess the ordering and the preservation of the porphyrin electronic structure at the interface with the substrate.

2. Results and Discussion

2.1. Structural Analysis

The LEED patterns observed for the Pd(001)-$p(1\times1)$ phase as well as the above described UTMO superstructures confirmed the high quality of substrate preparation. As observed in **Figure** 1A, a sharp and bright square diffraction pattern (black circled diffraction spots) obtained from the clean Pd(001)-$p(1\times1)$ substrate confirmed the absence of any surface contamination. The sharp and bright straight $p(2\times2)$ and rotated $p(\sqrt{5}\times\sqrt{5})$R27° patterns of the two UTMO superstructures of Pd [Figure 1B,C, respectively] were corroborated with the respective simulated diffraction patterns shown in the Supporting Information (Figure S1, Supporting Information). The yellow circled LEED spots reported in Figure 1C are the diffraction spots that confirm the presence of a single layer of Pd oxide, or alternatively,

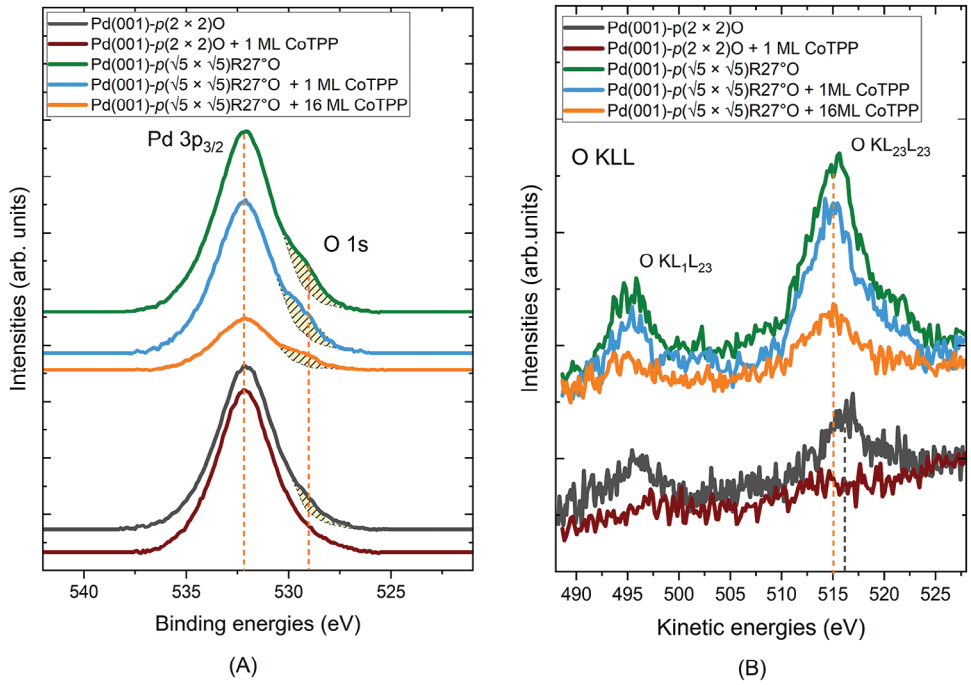

Figure 2. A) Core-level Pd $3p_{3/2}$/O 1s overlapping XPS peak region, and B) Auger O KLL XPS peak region, acquired with Mg Kα ($h\nu$ = 1253.6 eV) emission line, for the UTMO superstructures of Pd and the subsequent CoTPP depositions.

the $p(\sqrt{5} \times \sqrt{5})$R27°O phase, in agreement with the literature.[38–41] After the deposition of 1 ML CoTPP on each of these substrates, it was observed that molecular surface reconstruction takes place only in the case of CoTPP/Pd(001)-p($\sqrt{5} \times \sqrt{5}$)R27°O system as seen in Figure 1D. This resulting bright reconstruction is interpreted as the superposition of a straight (5 × 5) and rotated (5 × 5)R37° pattern[25] with comparable LEED spot intensities, in very good agreement with the ordered superstructures observed with tetraphenyl porphyrin deposition on Fe(001)-$p(1 \times 1)$O.[18–22,25]

2.2. Chemical State Analysis

The chemical analysis of the clean Pd(001)-$p(1 \times 1)$ substrate, the surface UTMO superstructures and the respective porphyrin depositions can be categorized into analysis of the characteristic XPS features arising from a) the substrate, with transitions Pd 3p, O 1s, and O KLL, and b) the porphyrin overlayer, with transitions C 1s, N 1s and Co 2p. Prior to porphyrin depositions, all substrates have been checked for C and N contamination and none has been found. Furthermore, the thick CoTPP film has been considered as a sample representative of CoTPP molecules not in contact with the substrate.[13,14,23]

2.2.1. XPS Substrate Analysis: Pre and Post Molecule Deposition

The analysis of the UTMO superstructures of Pd and subsequent CoTPP depositions required core-level O 1s and corresponding O $KL_{23}L_{23}$ Auger peak acquisition as shown in **Figure 2**. An overlap between the O 1s and Pd $3p_{3/2}$ peaks [Figure 2A] clearly shows Pd $3p_{3/2}$ as the main peak with a BE position at 532.1 eV, while the O 1s peak presents itself as a shoulder (yellow shaded region) with a BE position approximately at 529.1 eV, except its absence noted in the spectrum of 1 ML CoTPP/Pd(001)-$p(2 \times 2)$O system. This O 1s peak in a Pd $3p_{3/2}$/O 1s overlapping region has been identified in previous works[42–44] to be originating from an O-terminated PdO surface. It is to be noted that this O-shoulder is very prominent at the Pd(001)-$p(\sqrt{5} \times \sqrt{5})$R27°O and 1 ML CoTPP/Pd(001)-$p(\sqrt{5} \times \sqrt{5})$R27°O surfaces, and even at the thick CoTPP/Pd(001)-$p(\sqrt{5} \times \sqrt{5})$R27°O surface. The deposition of 1 ML CoTPP (light blue spectrum) does not significantly alter Pd and O-shoulder intensity, as expected for the attenuation provided by a monolayer of molecules. Obviously, when the amount of porphyrin molecules increases (16 ML; orange spectrum), the reduction of the Pd and O-shoulder intensity is clearly observed. However, the Pd:O relative intensity is roughly the same. This observation brings us to the interpretation that in the case of a CoTPP monolayer on Pd(001)-$p(\sqrt{5} \times \sqrt{5})$R27°O, the O atoms remain buried at the organic/inorganic interface and remain bonded to Pd below the porphyrin film, much like in the case of a monolayer of ZnTPP on Fe(001)-$p(1 \times 1)$O,[13] which is a necessary characteristic of the decoupling interlayer. The measured O KLL Auger peaks in Figure 2B, offer additional data on possible surface chemical modifications. First of all, the O $KL_{23}L_{23}$ peak intensities reiterate the corresponding attenuation observed in the O 1s peaks of Figure 2A. Secondly, the O $KL_{23}L_{23}$ peak with a KE position at 515.0 eV remains unchanged for the Pd(001)-$p(\sqrt{5} \times \sqrt{5})$R27°O, 1 ML CoTPP/Pd(001)-$p(\sqrt{5} \times \sqrt{5})$R27°O and 16 ML CoTPP/Pd(001)-$p(\sqrt{5} \times \sqrt{5})$R27°O surfaces, as expected from O atoms that remain stable at the interface.

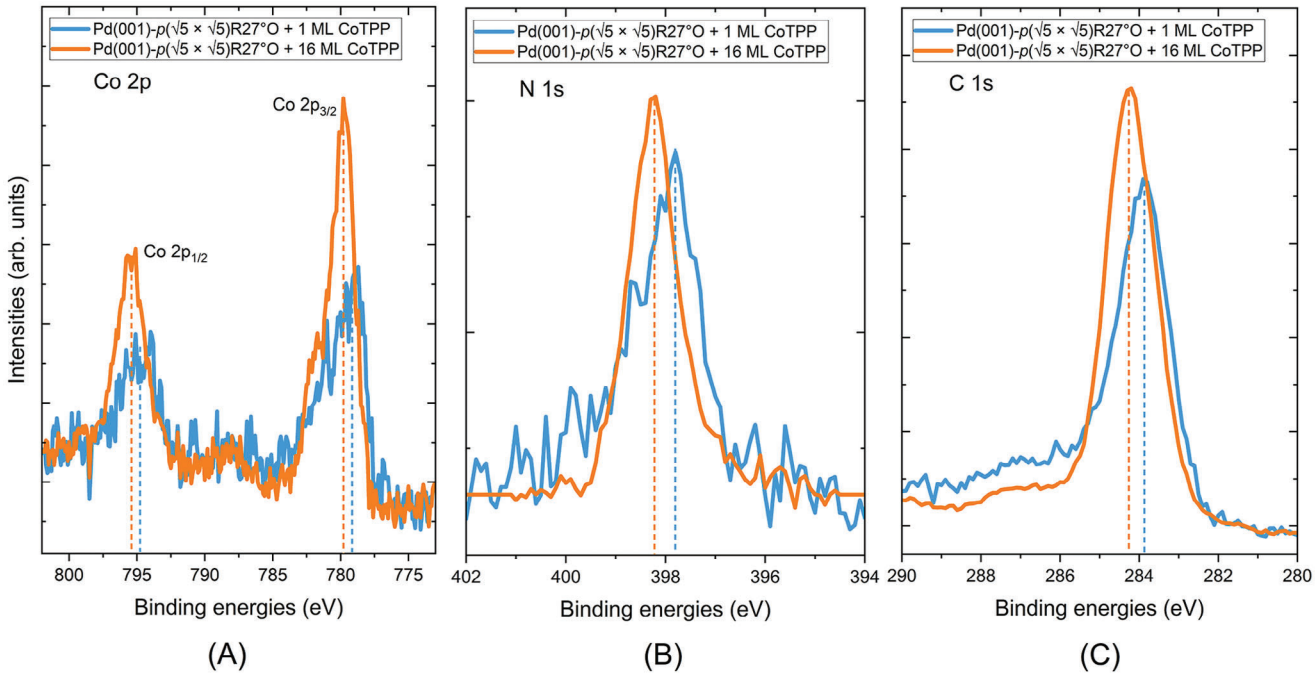

Figure 3. Core-level A) Co 2p, B) N 1s, and C) C 1s XPS peak regions, acquired with Mg Kα ($h\nu$ = 1253.6 eV) emission line, for the CoTPP depositions on the Pd(001)-$p(\sqrt{5} \times \sqrt{5})$R27°O superstructure.

This picture is different on the Pd(001)-$p(2 \times 2)$O surface. Indeed, the appearance of a smaller O-shoulder [yellow shaded region in Figure 2A] is a consequence of the lower concentration of O atoms at the surface. The O 1s peak is completely lacking at the 1 ML CoTPP/Pd(001)-$p(2 \times 2)$O surface (brown spectrum), suggesting an instability of the O interface (and a consequent possible O desorption) between Pd and the molecular film. For what concerns the O KLL Auger peaks in Figure 2B, a shift of 1.2 eV toward higher kinetic energies has been observed: this is proof of different configurations of O atoms on the first layer of Pd(001) lattice of this UTMO phase. The 1 ML CoTPP/Pd(001)-$p(2 \times 2)$O surface shows no discernible O $KL_{23}L_{23}$ peak formation, in agreement with the missing O 1s core-level peak, confirming the above mentioned instability of the O interface. As a consequence, CoTPP molecules are directly exposed to Pd atoms [as in the case of CoTPP deposition on clean Pd(001)-$p(1 \times 1)$], and the possible strong interaction precludes the formation of a well-ordered superstructure (absence of a LEED pattern). Hence this substrate does not serve our purpose and in the next section onward we focus our discussion only on the CoTPP/Pd(001)-$p(\sqrt{5} \times \sqrt{5})$R27°O system. All photoemission spectroscopic data for the CoTPP/Pd(001)-$p(1 \times 1)$ and CoTPP/Pd(001)-$p(2 \times 2)$O systems have been reported in the Supporting Information (Figures S2 and S3, Supporting Information).

2.2.2. XPS Analysis of the Molecular Film

The chemical structure of CoTPP is such that four peripheral phenyl (Ph) groups (24 C atoms) are linked to the main cavity of the molecule called a macrocycle, in the center of which is an almost flat tetrapyrrole ring (TPR) (16 pyrrolic C atoms, 4 imidic C atoms, 4 N atoms). The Co^{2+} metal ion is located in the center of the TPR. The respective XPS peaks are shown in **Figure 3**.

What we observe here is just a shift in binding energies of the main features in going from the 1ML CoTPP to the 16 ML thick CoTPP film. This shift of the core-level peaks in the porphyrin molecules may be attributed to a core hole polarization screening during the photoemission process and other electrostatic interactions at the molecule/substrate interface, whose effect is also prevalent in the valence states as highlighted in the following section. However, the overall line shapes are similar, and are compatible with literature data acquired on thick MTPP layers[45] suggesting a low interaction with the substrate for 1 ML CoTPP/Pd(001)-$p(\sqrt{5} \times \sqrt{5})$R27°O. This indicates that a monolayer of CoTPP on Pd(001)-$p(\sqrt{5} \times \sqrt{5})$R27°O substrate is similar in chemical environment to a thick CoTPP film, thus proving again the functioning of a Pd(001)-$p(\sqrt{5} \times \sqrt{5})$R27°O substrate as a decoupling interlayer.

2.3. Electronic Structure Analysis

In **Figure 4**, the UPS spectra of the valence states of the clean Pd(001)-$p(1 \times 1)$ substrate, the Pd(001)-$p(\sqrt{5} \times \sqrt{5})$R27°O superstructure, and the CoTPP monolayer on Pd(001)-$p(\sqrt{5} \times \sqrt{5})$R27°O are reported. As also considered for the XPS analysis, a thick CoTPP film grown on the Pd(001)-$p(\sqrt{5} \times \sqrt{5})$R27°O substrate has been considered as a sample representative of CoTPP molecules not interacting with Pd. Therefore, the corresponding UPS spectrum (orange) shows the main molecular features of the thick 16 ML CoTPP film with BE positions at 1.3 eV (HOMO), 3.4 eV (Ph_1), 4.9 eV (TPR) and 6.3 eV (Ph_2) w.r.t the Fermi edge (E_F) at 0 eV.[18,21,46] The HOMO level is a TPR

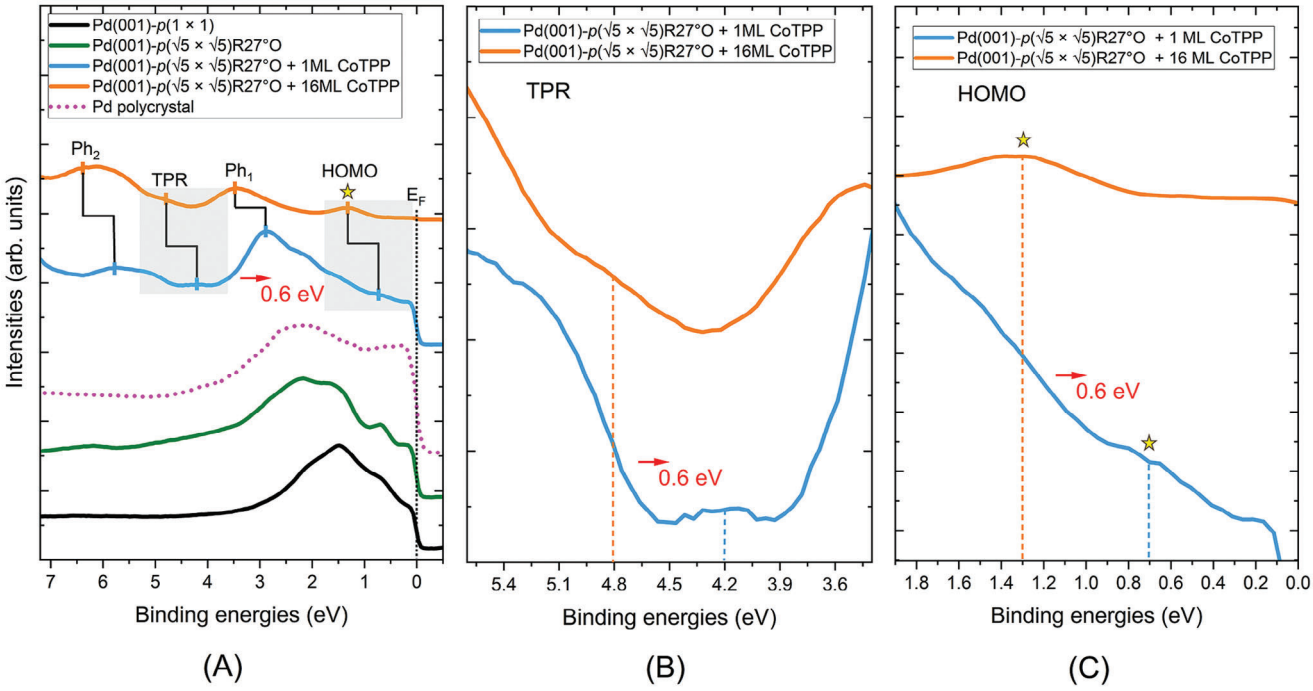

Figure 4. A) UPS valence band spectra, acquired with He I ($h\nu = 21.2$ eV) emission line, for the clean Pd(001)-$p(1 \times 1)$ substrate, the Pd(001)-$p(\sqrt{5} \times \sqrt{5})$R27°O superstructure and the CoTPP depositions on it. A Pd polycrystal UPS spectrum has been reproduced with permission.[49] 1993, Elsevier. The gray highlighted regions are the B) TPR and C) HOMO energetic regions for the CoTPP depositions, displayed for better peak visibility.

feature and here it is marked by a star. The following are some general comments stemming from the comparison of the line shape of all the valence band spectra depicted in Figure 4A. The clean Pd(001)-$p(1 \times 1)$ (black spectrum) is in good agreement with the literature.[47] The addition of O results in a specific line shape for the Pd(001)-$p(\sqrt{5} \times \sqrt{5})$R27°O superstructure (green spectrum). The addition of 1 ML CoTPP on Pd(001)-$p(\sqrt{5} \times \sqrt{5})$R27°O significantly affects the measured line shape (light blue spectrum). But such an observation is not unexpected because the substrate features might be perturbed by the scattering effect from the CoTPP molecular film, which can alter the line shape contribution from the underlying substrate.[46,48] Therefore, for a correct interpretation of the 1 ML CoTPP/Pd(001)-$p(\sqrt{5} \times \sqrt{5})$R27°O spectrum, a UPS spectrum of polycrystalline Pd (magenta spectrum) has been adapted from and reproduced with permission from Ref. [49] For what concerns the molecular features, some peaks are clearly visible at 2.8 eV (Ph_1) and 5.7 eV (Ph_2). We attribute Ph_1 and Ph_2 to photoemission from the porphyrin phenyl groups by comparison with the spectrum from the 16 ML thick CoTPP film, although with a shift toward lower binding energies (≈0.6 eV). This shift, already commented in the previous section, has also been observed in our previous work with ZnTPP and CoTPP molecules on Fe(001)-$p(1 \times 1)$O substrate[13,14,18,21] as well as for some other organic/inorganic interfaces.[15,46,50,51] By assuming the same energy shift, the remaining features on the 1 ML CoTPP/Pd(001)-$p(\sqrt{5} \times \sqrt{5})$R27°O spectrum, related to the TPR [detail in Figure 4B] and the HOMO [detail in Figure 4C], can be identified.

In **Figure 5**, the UPS spectra have been displayed in combination with the IPES spectra for unoccupied electronic states in order to complete the electronic levels picture. The IPES spectra for bare substrates Pd(001)-$p(1 \times 1)$ (black spectrum) and the Pd(001)-$p(\sqrt{5} \times \sqrt{5})$R27°O (green spectrum) are very similar. In particular, the result for clean Pd(001)-$p(1 \times 1)$ is in agreement with the available literature.[52] The IPES spectrum for the 16 ML thick CoTPP film (orange spectrum) shows the main molecular features with BE positions at 2.2 eV (LUMO) and 4.4 eV (Ph^*) w.r.t the E_F at 0 eV. Both HOMO and LUMO levels are marked by star symbols in their respective spectra. Observing the line shapes of all the IPES spectra, it is clear that 1 ML CoTPP/Pd(001)-$p(\sqrt{5} \times \sqrt{5})$R27°O (light blue spectrum) and 16 ML CoTPP/Pd(001)-$p(\sqrt{5} \times \sqrt{5})$R27°O (orange spectrum) share a similar line shape. In addition to these molecular features, the 1 ML CoTPP/Pd(001)-$p(\sqrt{5} \times \sqrt{5})$R27°O spectrum shows another feature at 0.4 eV w.r.t the E_F, which is the substrate contribution from the Pd(001)-$p(\sqrt{5} \times \sqrt{5})$R27°O substrate (green spectrum) and which is also attenuated after 1 ML CoTPP deposition. The HOMO-LUMO energy gap or band gap (E_g) values for the thick CoTPP film and at the 1 ML CoTPP/Pd(001)-$p(\sqrt{5} \times \sqrt{5})$R27°O interface obtained from combining the respective HOMO and LUMO BE positions w.r.t the E_F are 3.5 and 2.9 eV, respectively. The evolution of the electronic levels from the thick porphyrin film to a monolayer deposition on the Pd(001)-$p(\sqrt{5} \times \sqrt{5})$R27°O substrate shows a slight E_g shrinking at the CoTPP/Pd(001)-$p(\sqrt{5} \times \sqrt{5})$R27°O interface, consistent with similar observations on other organic/inorganic interfaces.[13–15,18,21,46,51]

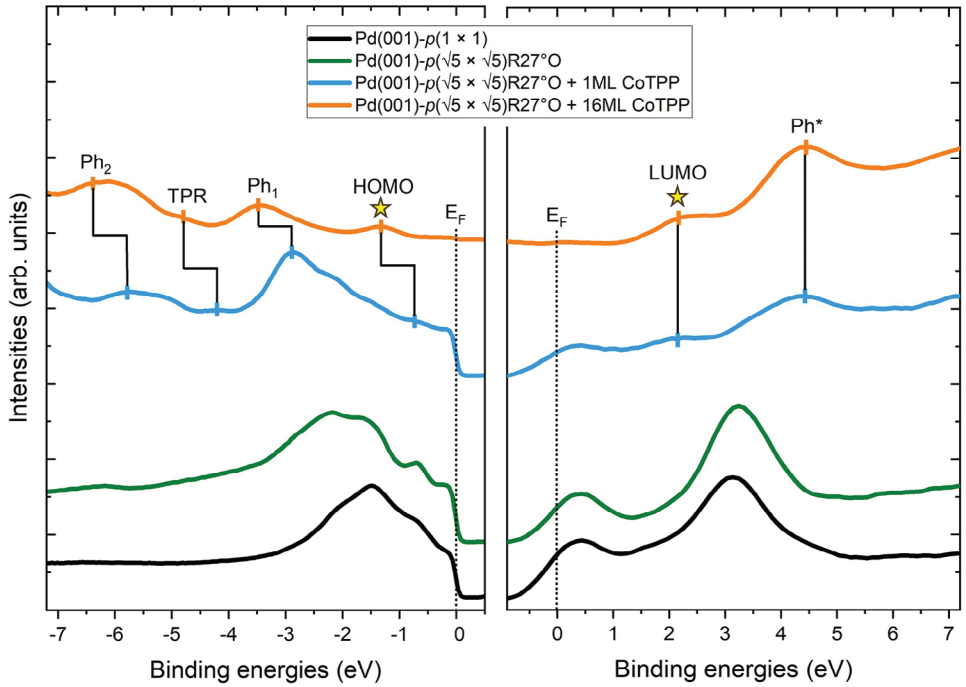

Figure 5. Combined UPS (left panel) and IPES (right panel) spectra for presentation of occupied and unoccupied electronic states in Pd(001)-$p(1 \times 1)$ and Pd(001)-$p(\sqrt{5} \times \sqrt{5})$R27°O substrates and the CoTPP depositions on Pd(001)-$p(\sqrt{5} \times \sqrt{5})$R27°O.

3. Conclusion

The organic molecule/metal heterojunction in organic electronic device preparation poses a major challenge that involves minimizing the molecule/substrate interaction. The concept of the use of a decoupling interlayer (i.e., a layer interposed between the metal substrate and the deposited organic molecules) is a topic of ongoing research and hence motivated our investigation.

In this work, we have studied the potential utilization of two UTMO phases of Pd(001) as passivation or decoupling interlayers for unperturbed organic molecule deposition. From a structural point of view, we succeeded to grow an ordered porphyrin superstructure in 1 ML CoTPP/Pd(001)-p$(\sqrt{5} \times \sqrt{5})$R27°O, in perfect agreement with 1 ML CoTPP/Fe(001)-p(1×1)O, despite a reduced amount (≈20% less) of O atoms at the interface. From a chemical point of view, the O atoms remain buried at this CoTPP/Pd(001)-p$(\sqrt{5} \times \sqrt{5})$R27°O interface. From an electronic point of view, the HOMO and LUMO levels of CoTPP can be identified also on a monolayer of molecules. This occurrence is a signature of the electronic integrity of the molecular TPR, even when in direct contact with the substrate.

These findings confirm the presence of a lower concentration limit for the effectiveness of O screening at the interface, which in the present case settles at ≈0.80 ML. On the other end, at ≈0.25 ML O concentration, the stability of the O interface is lost and 1 ML CoTPP molecules are exposed to the bare Pd surface, which precludes both the formation of an ordered structure and the electronic integrity of the molecular film. In conclusion, the above analysis evidences significant similarities of the Pd(001)-$p(\sqrt{5} \times \sqrt{5})$R27°O surface with the already established Fe(001)-p(1×1)O surface working as a passivation interlayer and opens the scope for future investigation such as its testing on other organic molecules relevant for device electronics.

4. Experimental Section

Sample Preparation: Sample preparation began in an ultra-high vacuum (UHV) system (base pressure in high 10^{-11} Torr) with a polished Pd single crystal substrate Pd(001) purchased from the Surface Preparation Laboratory. The clean Pd(001)-$p(1 \times 1)$ substrate was obtained following this protocol: a) Ar^+ sputtering of the Pd(001) substrate at a beam voltage of 1.5 kV and a beam current of 2 μA for 20 min while the chamber stays at an Ar pressure of low 10^{-8} Torr, b) exposure to 4.7 L of O_2 (partial pressure of 2.6×10^{-8} Torr, exposure time of 3 min) with substrate kept at 630 °C, c) higher temperature annealing at 730 °C of the sample for 3 min for excess O removal from the surface while the chamber being at low 10^{-9} Torr pressure. The low O coverage Pd(001)-$p(2 \times 2)$O substrate was prepared by exposing the clean Pd(001)-$p(1 \times 1)$ substrate to 240 L of O_2 with the substrate at room temperature (RT). The high O coverage Pd(001)-$p(\sqrt{5} \times \sqrt{5})$R27°O substrate was prepared as follows: a) exposure of the Pd(001)-$p(2 \times 2)$O substrate (see above) to 144 L of O_2 with the substrate kept at 200 °C, b) exposure of the sample to 480 L of O_2 keeping the substrate at 300 °C. **Figure 6** shows a schematic summary of the preparation of the $p(1 \times 1)$ phase at RT as well as the above described UTMO superstructures of Pd as functions of O_2 exposure and substrate temperature.

The above described Pd(001)-$p(1 \times 1)$, Pd(001)-$p(2 \times 2)$O, and Pd(001)-$p(\sqrt{5} \times \sqrt{5})$R27°O substrate preparations were each followed by the deposition of organic molecules in a dedicated vacuum chamber by means of organic molecular beam epitaxy (OMBE). CoTPP molecules, purchased from Merck, were sublimated by means of a Knudsen effusion cell. Before sublimation on the substrates, CoTPP was separately degassed in a vacuum. CoTPP were deposited at an evaporation temperature of ≈300 °C,

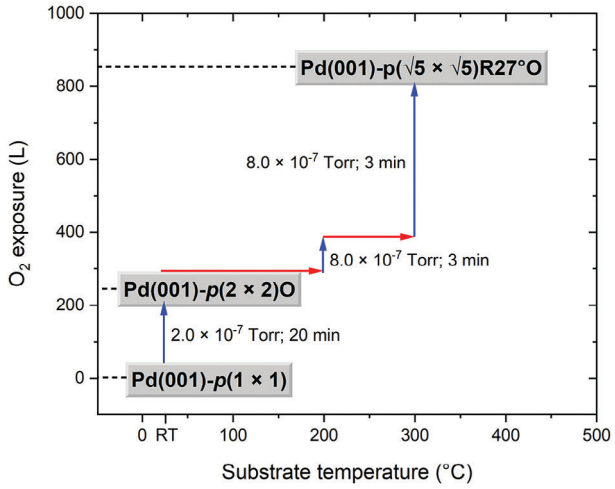

Figure 6. Summary of the prepared UTMO superstructures of Pd: Pd(001)-$p(2 \times 2)$O and Pd(001)-$p(\sqrt{5} \times \sqrt{5})$R27°O, as functions of O_2 exposure and substrate temperature. This schematic also summarizes the preparation flowchart of these two UTMO superstructures starting from clean Pd(001)-$p(1 \times 1)$ kept at RT. The blue arrows indicate changes in O_2 exposure while the red arrows indicate changes in substrate temperature.

depending on prior calibration of the effusion rate of the cell. Temperature controllers stabilize the cell crucible heating temperatures within 0.5 °C. The CoTPP deposition rate was monitored by a quartz microbalance that enabled one to maintain a rate of ≈1 Å min^{-1}. A complete monolayer coverage of CoTPP molecules corresponds to a film thickness of ≈3.06 Å.[12,13] All CoTPP films were grown with the substrates kept at RT and up to the nominal thicknesses of a monolayer. Additionally, a thick CoTPP film (16 ML) thickness was grown on the Pd(001)-$p(\sqrt{5} \times \sqrt{5})$R27°O substrate at RT, to obtain photoemission spectra representative of CoTPP molecules not in contact with the Pd substrate.

Sample Characterization: LEED was acquired on samples with the $p(1 \times 1)$ phase and the above described UTMO superstructures. LEED images were taken at an incident beam energy of 55 eV and with substrates always kept at RT, before and after the PES characterizations, by exposing the sample to the electron beam for a few seconds. LEED patterns observed in the experiments have been corroborated with simulated diffraction patterns produced by the software LEEDpat.[53] All the samples were characterized at RT by XPS and UPS, which were performed utilizing non-monochromatized radiations, Mg Kα ($h\nu$ = 1253.6 eV) and He I ($h\nu$ = 21.2 eV), respectively. Additionally, XPS and UPS were performed on the thick CoTPP film grown on the Pd(001)-$p(\sqrt{5} \times \sqrt{5})$R27°O substrate. Photoelectrons were collected at normal emission by a 150 mm hemispherical electron analyzer (SPECS GmbH),[12] providing an overall (electron + photon) full width at half maximum (FWHM) energy resolution of ≈0.9 eV and 30 meV for XPS and UPS, respectively. All acquired core-level XPS peaks and UPS spectra have been subjected to satellite peak removal. Some of the samples were further characterized by IPES. The home-made IPES system employs a GaAs(001) crystal covered by Cs oxide as the photocathode. Generated electrons impinge the sample at normal incidence. The IPES setup was operated in isochromatic mode, i.e., by changing the energy of the impinging electrons and detecting 9.6 eV inverse photoemission photons with a bandpass detector.[54–56] The FWHM energy resolution of IPES is ≈0.7 eV.

Supporting Information

Supporting Information is available from the Wiley Online Library or from the author.

Acknowledgements

The present work has been undertaken under the project MOX-OPIF – METAL OXIDE/ORGANIC PASSIVATED INTERFACES: IMPLICATIONS FOR ORGANIC ELECTRONICS with project code (CUP) D43C22004190001 and grant from the Young Researchers Marie Skłodowska-Curie Action (MSCA) Seal of Excellence (SoE) Research Grant with protocol no. SOE_0000076 awarded by the Ministero dell'Università e della Ricerca (MUR), Italy. The Marie Skłodowska-Curie Action (MSCA) Seal of Excellence (SoE) Individual Fellowship 2020 project with project code (CUP) D45F21005290001 and grant no. UA.A.RRR.DFIS.PAMM.STUD.BGP1VARI01 awarded by Politecnico di Milano, Italy, is also acknowledged. G. Albani is thanked for fruitful discussions.

Conflict of Interest

The authors declare no conflict of interest.

Author Contributions

I.M. performed conceptualization, formal analysis, investigation, methodology, and wrote the original draft, reviewed and performed editing of the manuscript. F.G. performed formal analysis, investigation, and methodology. A.C. performed conceptualization, supervision, and reviewed and performed editing of the manuscript. L.D. and F.C. performed supervision, and reviewed and performed editing of the manuscript. G.B. performed conceptualization, supervision, validation, acquired resources, and reviewed and performed editing of the manuscript.

Data Availability Statement

The data that support the findings of this study are available from the corresponding author upon reasonable request.

Keywords

materials science, nanotechnology, organic/metal interfaces, photoemission spectroscopy, thin films

Received: May 21, 2024
Revised: August 6, 2024
Published online: August 26, 2024

[1] J. Shalf, *Philos. Trans. R. Soc. London, Ser A* **2020**, *378*, 20190061.
[2] S. Forrest, P. Burrows, M. Thompson, *IEEE Spectrum* **2000**, *37*, 29.
[3] C. Liao, M. Zhang, M. Y. Yao, T. Hua, L. Li, F. Yan, *Adv. Mater.* **2015**, *27*, 7493.
[4] S. R. Forrest, M. E. Thompson, *Chem. Rev.* **2007**, *107*, 923.
[5] N. Xin, J. Guan, C. Zhou, X. Chen, C. Gu, Y. Li, M. A. Ratner, A. Nitzan, J. F. Stoddart, X. Guo, *Nat. Rev. Phys.* **2019**, *1*, 211.
[6] W. Hieringer, K. Flechtner, A. Kretschmann, K. Seufert, W. Auwärter, J. V. Barth, A. Görling, H.-P. Steinrück, J. M. Gottfried, *J. Am. Chem. Soc.* **2011**, *133*, 6206.
[7] B. Han, Y. Li, X. Ji, X. Song, S. Ding, B. Li, H. Khalid, Y. Zhang, X. Xu, L. Tian, H. Dong, X. Yu, W. Hu, *J. Am. Chem. Soc.* **2020**, *142*, 9708.
[8] R. Bertacco, F. Ciccacci, *Phys. Rev. B: Condens. Matter Mater. Phys.* **1999**, *59*, 4207.
[9] A. Picone, A. Brambilla, A. Calloni, L. Duo', M. Finazzi, F. Ciccacci, *Phys. Rev. B: Condens. Matter Mater. Phys.* **2011**, *83*, 235402.

[10] A. Picone, G. Bussetti, M. Riva, A. Calloni, A. Brambilla, L. Duò, F. Ciccacci, M. Finazzi, *Phys. Rev. B: Condens. Matter Mater. Phys.* **2012**, *86*, 075465.
[11] A. Brambilla, A. Calloni, A. Picone, M. Finazzi, L. Duò, F. Ciccacci, *Appl. Surf. Sci.* **2013**, *267*, 141.
[12] G. Berti, A. Calloni, A. Brambilla, G. Bussetti, L. Duò, F. Ciccacci, *Rev. Sci. Instrum.* **2014**, *85*, 073901.
[13] G. Bussetti, A. Calloni, M. Celeri, R. Yivlialin, M. Finazzi, F. Bottegoni, L. Duò, F. Ciccacci, *Appl. Surf. Sci.* **2016**, *390*, 856.
[14] G. Bussetti, A. Calloni, R. Yivlialin, A. Picone, F. Bottegoni, M. Finazzi, *Beilstein J. Nanotechnol.* **2016**, *7*, 1527.
[15] A. Picone, D. Gianotti, M. Riva, A. Calloni, G. Bussetti, G. Berti, L. Duò, F. Ciccacci, M. Finazzi, A. Brambilla, *ACS Appl. Mater. Interfaces* **2016**, *8*, 26418.
[16] A. Calloni, G. Fratesi, S. Achilli, G. Berti, G. Bussetti, A. Picone, A. Brambilla, P. Folegati, F. Ciccacci, L. Duò, *Phys. Rev. B: Condens. Matter Mater. Phys.* **2017**, *96*, 085427.
[17] A. Picone, D. Giannotti, A. Brambilla, G. Bussetti, A. Calloni, R. Yivlialin, M. Finazzi, L. Duò, F. Ciccacci, A. Goldoni, A. Verdini, L. Floreano, *Appl. Surf. Sci.* **2018**, *435*, 841.
[18] M. S. Jagadeesh, A. Calloni, A. Brambilla, A. Picone, A. Lodesani, L. Duò, F. Ciccacci, G. Bussetti, *Appl. Phys. Lett.* **2019**, *115*, 082404.
[19] G. Albani, A. Calloni, M. S. Jagadeesh, M. Finazzi, L. Duò, F. Ciccacci, G. Bussetti, *J. Appl. Phys.* **2020**, *128*, 035501.
[20] A. Calloni, M. S. Jagadeesh, G. Albani, C. Goletti, L. Duò, F. Ciccacci, G. Bussetti, in *EPJ Web of Conf.*, Italian National Conf. on the Phys. of Matter (FisMat 2019), Catania, Italy **2020**, https://doi.org/10.1051/epjconf/202023000014.
[21] A. Calloni, M. S. Jagadeesh, G. Bussetti, G. Fratesi, S. Achilli, A. Picone, A. Lodesani, A. Brambilla, C. Goletti, F. Ciccacci, L. Duò, M. Finazzi, A. Goldoni, A. Verdini, L. Floreano, *Appl. Surf. Sci.* **2020**, *505*, 144213.
[22] G. Fratesi, S. Achilli, A. Ugolotti, A. Lodesani, A. Picone, A. Brambilla, L. Floreano, A. Calloni, G. Bussetti, *Appl. Surf. Sci.* **2020**, *530*, 147085.
[23] G. Albani, A. Calloni, A. Picone, A. Brambilla, M. Capra, A. Lodesani, L. Duò, M. Finazzi, F. Ciccacci, G. Bussetti, *Micromachines* **2021**, *12*, 191.
[24] G. Albani, M. Capra, A. Lodesani, A. Calloni, G. Bussetti, M. Finazzi, F. Ciccacci, A. Brambilla, L. Duò, A. Picone, *Beilstein J. Nanotechnol.* **2022**, *13*, 857.
[25] I. Majumdar, F. Goto, A. Calloni, G. Albani, L. Duò, M. Finazzi, F. Ciccacci, G. Bussetti, *Appl. Surf. Sci.* **2023**, *636*, 157807.
[26] A. Orbelli-Biroli, A. Calloni, A. Bossi, M. S. Jagadeesh, G. Albani, L. Duò, F. Ciccacci, A. Goldoni, A. Verdini, L. Schio, L. Floreano, G. Bussetti, *Adv. Funct. Mater.* **2021**, *31*, 2011008.
[27] M. Jurow, A. E. Schukman, J. D. Batteas, C. M. Drain, *Coord. Chem. Rev.* **2010**, *254*, 2297.
[28] G. Bussetti, G. Albani, A. Calloni, M. S. Jagadeesh, C. Goletti, L. Duò, F. Ciccacci, *Appl. Surf. Sci.* **2020**, *514*, 145891.
[29] M. M. Montemore, M. A. van Spronsen, R. J. Madix, C. M. Friend, *Chem. Rev.* **2018**, *118*, 2816.
[30] T. W. Orent, S. D. Bader, *Surf. Sci.* **1982**, *115*, 323.
[31] S.-L. Chang, P. A. Thiel, *Phys. Rev. Lett.* **1987**, *59*, 296.
[32] S.-L. Chang, P. A. Thiel, *J. Chem. Phys.* **1988**, *88*, 2071.
[33] S.-L. Chang, P. A. Thiel, *Surf. Sci.* **1988**, *205*, 117.
[34] G. W. Simmons, Y.-N. Wang, J. Marcos, K. Klier, *J. Phys. Chem.* **1991**, *95*, 4522.
[35] M. Lahti, A. Puisto, M. Alatalo, T. S. Rahman, *Surf. Sci.* **2008**, *602*, 3660.
[36] A. den Dunnen, S. Wiegman, L. Jacobse, L. B. F. Juurlink, *J. Chem. Phys.* **2015**, *142*, 214708.
[37] A. den Dunnen, L. Jacobse, S. Wiegman, O. T. Berg, L. B. F. Juurlink, *J. Chem. Phys.* **2016**, *144*, 244706.
[38] V. Mehar, M. Kim, M. Shipilin, M. Van den Bossche, J. Gustafson, L. R. Merte, U. Hejral, H. Grönbeck, E. Lundgren, A. Asthagiri, J. F. Weaver, *ACS Catal.* **2018**, *8*, 8553.
[39] M. Todorova, E. Lundgren, V. Blum, A. Mikkelsen, S. Gray, J. Gustafson, M. Borg, J. Rogal, K. Reuter, J. N. Andersen, M. Scheffler, *Surf. Sci.* **2003**, *541*, 101.
[40] P. Kostelnik, N. Seriani, G. Kresse, A. Mikkelsen, E. Lundgren, V. Blum, T. Šikola, P. Varga, M. Schmid, *Surf. Sci.* **2007**, *601*, 1574.
[41] M. Shipilin, A. Stierle, L. R. Merte, J. Gustafson, U. Hejral, N. M. Martin, C. Zhang, D. Franz, V. Kilic, E. Lundgren, *Surf. Sci.* **2017**, *660*, 1.
[42] H. Gabasch, W. Unterberger, K. Hayek, B. Klötzer, E. Kleimenov, D. Teschner, S. Zafeiratos, M. Hävecker, A. Knop-Gericke, R. Schlögl, J. Han, F. H. Ribeiro, B. Aszalos-Kiss, T. Curtin, D. Zemlyanov, *Surf. Sci.* **2006**, *600*, 2980.
[43] D. Zemlyanov, B. Klötzer, H. Gabasch, A. Smeltz, F. H. Ribeiro, S. Zafeiratos, D. Teschner, P. Schnörch, E. Vass, M. Hävecker, A. Knop-Gericke, R. Schlögl, *Top. Catal.* **2013**, *56*, 885.
[44] C. Hartwig, K. Schweinar, R. Nicholls, S. Beeg, R. Schlögl, M. Greiner, *J. Chem. Phys.* **2021**, *154*, 174708.
[45] C. Castellarin Cudia, T. Caruso, E. Maccallini, A. Li Bassi, P. Carrozzo, O. De Luca, A. Goldoni, V. Lyamayev, K. C. Prince, F. Bondino, E. Magnano, R. G. Agostino, C. S. Casari, *J. Phys. Chem. C* **2015**, *119*, 8671.
[46] F. Goto, A. Calloni, I. Majumdar, R. Yivlialin, C. Filoni, C. Hogan, M. Palummo, A. Orbelli-Biroli, M. Finazzi, L. Duò, F. Ciccacci, G. Bussetti, *Inorg. Chim. Acta* **2023**, *556*, 121612.
[47] D. R. Lloyd, C. M. Quinn, N. V. Richardson, *Surf. Sci.* **1977**, *63*, 174.
[48] L. Giovanelli, F. C. Bocquet, P. Amsalem, H.-L. Lee, M. Abel, S. Clair, M. Koudia, T. Faury, L. Petaccia, D. Topwal, E. Salomon, T. Angot, A. A. Cafolla, N. Koch, L. Porte, A. Goldoni, J.-M. Themlin, *Phys. Rev. B: Condens. Matter Mater. Phys.* **2013**, *87*, 035413.
[49] T. Gouder, C. A. Colmenares, *Surf. Sci.* **1993**, *295*, 241.
[50] H. Peisert, A. Petershans, T. Chasse, *J. Phys. Chem. C* **2008**, *112*, 5703.
[51] C. Castellarin Cudia, P. Vilmercati, R. Larciprete, C. Cepek, G. Zampieri, L. Sangaletti, S. Pagliara, A. Verdini, A. Cossaro, L. Floreano, A. Morgante, L. Petaccia, S. Lizzit, C. Battocchio, G. Polzonetti, A. Goldoni, *Surf. Sci.* **2006**, *600*, 4013.
[52] J. Rogozik, J. Küppers, V. Dose, *Surf. Sci.* **1984**, *148*, L653.
[53] K. E. Hermann, M. A. Van Hove, LEEDpat4: LEED pattern analyzer, https://www.fhi.mpg.de/958975/LEEDpat4, (accessed: August 2024).
[54] F. Ciccacci, E. Vescovo, G. Chiaia, S. De Rossi, M. Tosca, *Rev. Sci. Instrum.* **1992**, *63*, 3333.
[55] M. Finazzi, A. Bastianon, G. Chiaia, F. Ciccacci, *Meas. Sci. Technol.* **1993**, *4*, 234.
[56] G. Chiaia, S. De Rossi, L. Mazzolari, F. Ciccacci, *Phys. Rev. B: Condens. Matter Mater. Phys.* **1993**, *48*, 11298.